

# On Episodes, Prototypical Networks, and Few-shot Learning

Steinar Laenen\*    Luca Bertinetto

`www.five.ai`

## Abstract

Episodic learning is a popular practice among researchers and practitioners interested in few-shot learning. It consists of organising training in a series of learning problems, each relying on small “support” and “query” sets to mimic the few-shot circumstances encountered during evaluation. In this paper, we investigate the usefulness of episodic learning in Prototypical Networks and Matching Networks, two of the most popular algorithms making use of this practice. Surprisingly, in our experiments we found that, for Prototypical and Matching Networks, it is detrimental to use the episodic learning strategy of separating training samples between support and query set, as it is a data-inefficient way to exploit training batches. These “non-episodic” variants, which are closely related to the classic Neighbourhood Component Analysis, reliably improve over their episodic counterparts in multiple datasets, achieving an accuracy that (in the case of Prototypical Networks) is competitive with the state-of-the-art, despite being extremely simple.

## 1 Introduction

The problem of few-shot learning (FSL) – classifying examples from previously unseen classes given only a handful of training data – has considerably grown in popularity within the machine learning community in the last few years. The reason is likely twofold. First, being able to perform well on FSL problems is important for several applications, from learning new characters (Lake et al., 2015) to drug discovery (Altae-Tran et al., 2017). Second, since the aim of researchers interested in meta-learning is to design systems that can quickly learn novel concepts by generalising from previously encountered learning tasks, FSL benchmarks are often adopted as a practical way to empirically validate meta-learning algorithms.

To the best of our knowledge, there is not a widely recognised definition of meta-learning. In a recent survey, Hospedales et al. (2020) informally describe it as “*the process of improving a learning algorithm over multiple learning episodes*”. Several popular papers in the FSL community (e.g. Vinyals et al. (2016); Ravi & Larochelle (2017); Finn et al. (2017); Snell et al. (2017)) have emphasised the importance of organising training into *episodes*, i.e. learning problems with a limited amount of training and pseudo-test examples that resemble the test-time scenario. This popularity has reached such a point that an “episodic” data-loader is often at the core of new FSL algorithms, a practice facilitated by frameworks such as Deleu et al. (2019) and Grefenstette et al. (2019).

Despite the considerable strides made in FSL over the past few years, several recent works (e.g. Chen et al. (2019); Wang et al. (2019); Dhillon et al. (2020); Tian et al. (2020)) showed that simple baselines can outperform established meta-learning methods by using embeddings pre-trained with standard classification losses. These results have cast a doubt in the FSL community on the usefulness of meta-learning and its pervasive episodes. Inspired by these results, we aim at understanding the practical usefulness of episodic learning in Prototypical Networks (Snell et al., 2017), one of the simplest and most

---

\*Correspondence to steinar9@gmail.com and luca.bertinetto@five.ai

popular methods which make use of it, and that has often inspired more recent methods (e.g. Oreshkin et al. (2018); Cao et al. (2020); Gidaris et al. (2019); Yoon et al. (2019); Cai et al. (2018)).

With a set of ablative experiments, we show that for Prototypical Networks episodic learning *a*) is detrimental for performance, *b*) is analogous to randomly discarding examples from a batch and *c*) it introduces a set of unnecessary hyperparameters that require careful tuning. Similar results are also obtained for Matching Networks, which is closely related to Prototypical Networks in the multi-shot case (and equivalent in the 1-shot case). Without episodic learning, Prototypical Networks and Matching Networks can be reduced to the classic *Neighbourhood Component Analysis* (NCA) (Goldberger et al., 2005; Salakhutdinov & Hinton, 2007) on deep embeddings and achieve, without bells and whistles, an accuracy that is competitive with the state-of-the-art on multiple FSL benchmarks: *miniImageNet*, *CIFAR-FS* and *tieredImageNet*.

Code will be made available at <https://github.com/fiveai/on-episodes-fsl>.

## 2 Related work

Pioneered by the seminal work of Utgoff (1986), Schmidhuber (1987, 1992), Bengio et al. (1992) and Thrun (1996), the general concept of meta-learning is several decades old (for a survey see Vilalta & Drissi (2002); Hospedales et al. (2020)). However, in the last few years it has experienced a surge in popularity, becoming the most used paradigm for learning from very few examples. Several methods addressing the FSL problem by learning on episodes were proposed. MANN (Santoro et al., 2016) uses a Neural Turing Machine (Graves et al., 2014) to save and access the information useful to meta-learn; Bertinetto et al. (2016) propose a deep network in which a “teacher” branch is tasked with predicting the parameters of a “student” branch; Matching Networks (Vinyals et al., 2016) and Prototypical Networks (Snell et al., 2017) are two non-parametric methods in which the contributions of different examples in the support set are weighted by either an LSTM or a softmax over the cosine distances for Matching Networks, and a simple average for Prototypical Networks; Ravi & Larochelle (2017) propose instead to use an LSTM to learn the hyperparameters of SGD, while MAML (Finn et al., 2017) learns to fine-tune an entire deep network by backpropagating through SGD. Despite these works widely differing in nature, they all stress on the importance of organising training in a series of small learning problems (*episodes*) that are similar to those encountered during inference at test time.

In contrast with this trend, a handful of papers have recently shown that simple approaches that forego episodes and meta-learning can perform well on FSL benchmarks. These methods all have in common that they pre-train a feature extractor with the cross-entropy loss on the “meta-training classes” of the dataset. Then, at test time a classifier is adapted to the support set by weight imprinting (Qi et al., 2018; Dhillon et al., 2020), fine-tuning (Chen et al., 2019), transductive fine-tuning (Dhillon et al., 2020) or logistic regression (Tian et al., 2020). Wang et al. (2019) suggest performing test-time classification by using the label of the closest centroid to the query image.

Different from these papers, we try to shed some light on one of the possible causes behind the poor performance of episodic-based algorithms like Prototypical Networks and Matching Networks. An analysis similar to ours in spirit is the one of Raghu et al. (2020). After showing that the efficacy of MAML in FSL is due to the adaptation of the final layer and the “reuse” of the features of previous layers, they propose a variant with the same accuracy and computational advantages. In this paper, we focus on FSL algorithms just as established, and uncover inefficiencies that not only allow for notable conceptual simplifications, but that also bring a significant boost in performance.

## 3 Background and method

This section is divided as follows: Sec. 3.1 introduces episodic learning and the formalism used in FSL, Sec. 3.2 reviews Prototypical Networks (often referred to as PNs from now on), Sec. 3.3 describes the classic NCA loss and how exactly it relates to PNs, and Sec. 3.4 explains the three options we explored to perform FSL classification with an NCA-trained feature embedding.

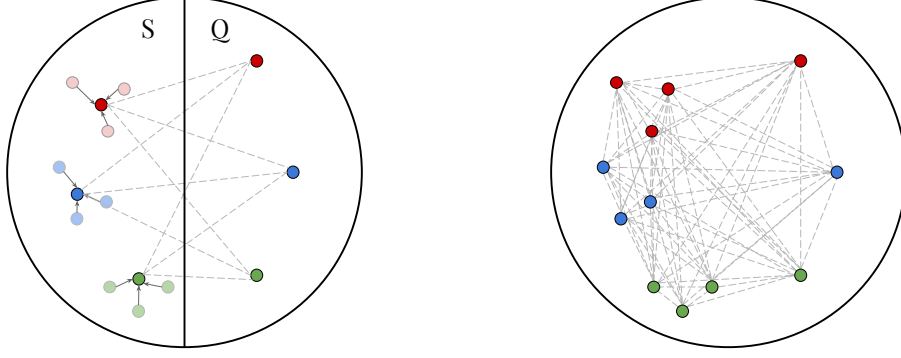


Figure 1: **Batch exploitation** during training for Prototypical Networks (Snell et al., 2017) (left) vs. Neighbourhood Component Analysis (Goldberger et al., 2005) (right) on a toy few-shot problem of 3 “ways”, 3 “shots” and 1 “query” per class. By dividing batches between support set  $S$  and query set  $Q$ , Prototypical Networks disregards many of the distances between labelled examples that would constitute useful training signal. Details in Sec. 3.3.

### 3.1 Episodic learning

A common strategy to train few-shot learning algorithms is to consider a distribution  $\hat{\mathcal{E}}$  over possible subsets of labels that is as close as possible to the one encountered during evaluation  $\mathcal{E}^1$ . Each episodic batch  $B_E = \{S, Q\}$  is obtained by first sampling a subset of labels  $L$  from  $\hat{\mathcal{E}}$ , and then sampling images constituting both *support set*  $S$  and *query set*  $Q$  from the set of images with labels in  $L$ , where  $S = \{(\mathbf{s}_1, y_1), \dots, (\mathbf{s}_n, y_n)\}$ ,  $Q = \{(\mathbf{q}_1, y_1), \dots, (\mathbf{q}_m, y_m)\}$ , and  $S_k$  and  $Q_k$  denote the sets of images with label  $y = k$  in the support set and query set respectively. In a Maximum Likelihood Estimation framework, training on these episodes can be written (Vinyals et al., 2016) as the optimisation

$$\arg \max_{\theta} E_{L \sim \hat{\mathcal{E}}} \left[ E_{S \sim L, Q \sim L} \left[ \sum_{(q_i, y_i) \in Q} \log P_{\theta}(y_i | q_i, S) \right] \right]. \quad (1)$$

In most implementations, this corresponds to training on a series of mini-batches in which each image belongs either to the support or the query set. Support and query sets are constructed such that they both contain all the classes of  $L$ , and a constant number of images per class. Therefore, episodes are characterised by three values: the number of classes  $w = |L|$  (the “ways”), the number of examples per class in the support set  $n = |S_k|$  (the “shots”), and the number of examples per class in the query set  $m = |Q_k|$ . Importantly, during evaluation the triplet  $\{w, n, m\}$  defines the problem setup. Usually, the triplet remains unchanged across methods, although the Meta-Dataset benchmark of Triantafillou et al. (2019) evaluates on episodes with a variable number of ways and shots. At training time, the triplet  $\{w, n, m\}$  can be seen as a set of hyperparameters controlling the batch creation, and that (as we will see in Sec. 4.2) requires careful tuning.

### 3.2 Prototypical Networks (PNs)

Prototypical Networks (Snell et al., 2017) are one of the most popular and effective approaches in the few-shot learning literature, and they are at the core of many newly-proposed methods (e.g. Oreshkin et al. (2018); Gidaris et al. (2019); Allen et al. (2019); Yoon et al. (2019); Cao et al. (2020)).

During *training*, episodes constituted by support set  $S$  and query set  $Q$  are sampled as described in Sec. 3.1. Then, a *prototype* for each class  $k$  is computed as the mean embedding of the samples from the support set belonging to that class:  $\mathbf{c}_k = (1/|S_k|) \cdot \sum_{(\mathbf{s}_i, y_k) \in S_k} f_{\theta}(\mathbf{s}_i)$ , where  $f_{\theta}$  is a deep neural networks with parameters  $\theta$  learned via Eq. 1.

<sup>1</sup>Note that, in FSL, the sets of classes of training and evaluation are disjoint.

	positives	negatives
PNs	$wmn$	$w(w-1)mn$
NCA	$\binom{m+n}{2}w$	$\binom{w}{2}(m+n)^2$

Table 1: Number of gradients from positive and negative distance pairs contributing to the loss within a batch. Respectively,  $w$ ,  $n$  and  $m$  represent the number of ways, shots and queries. In Appendix A.7 we show that the extra number of pairs that NCA can exploit in addition to PNs grows as  $O(w^2(m^2 + n^2))$ .

Let  $C = \{(\mathbf{c}_1, y_1), \dots, (\mathbf{c}_k, y_k)\}$  be the set of prototypes and corresponding labels. The loss can be written as follows:

$$\mathcal{L}_{\text{proto}}(S, Q) = -\frac{1}{|Q|} \sum_{(\mathbf{q}_i, y_i) \in Q} \log \left( \frac{\exp -\|f_\theta(\mathbf{q}_i) - \mathbf{c}_{y_i}\|^2}{\sum_{k'} \exp -\|f_\theta(\mathbf{q}_i) - \mathbf{c}_{k'}\|^2} \right). \quad (2)$$

Here,  $k'$  is an index that goes over all classes. This loss is minimised over a number of training episodes. After training, given a query image  $\mathbf{x}_i$  from a new test episode, classification is conducted by simply consulting the nearest-neighbouring prototype computed from the support set of the episode, i.e.  $y(\mathbf{x}_i) = \arg \min_{j \in \{1, \dots, k\}} \|f_\theta(\mathbf{x}_i) - \mathbf{c}_j\|$ .

### 3.3 Neighbourhood Component Analysis (NCA)

Eq. 2 computes the likelihood that a query image belongs to the class a certain prototype is representative of by computing the softmax over the distances to all prototypes. This formulation is similar to the *Neighbourhood Component Analysis* approach by Goldberger et al. (2005) (and expanded to the non-linear case by Salakhutdinov & Hinton (2007)), except for a few important differences which we will now discuss.

Let  $i \in [1, b]$  be the indices of the images within a batch  $B$ . The NCA loss can be written as:

$$\mathcal{L}_{\text{NCA}}(X) = -\frac{1}{b} \sum_{i \in 1, \dots, b} \log \left( \frac{\sum_{\substack{j \in 1, \dots, b \\ j \neq i \\ y_i = y_j}} \exp -\|\mathbf{z}_i - \mathbf{z}_j\|^2}{\sum_{\substack{k \in 1, \dots, b \\ k \neq i}} \exp -\|\mathbf{z}_i - \mathbf{z}_k\|^2} \right), \quad (3)$$

where  $\mathbf{z}_i = f_\theta(\mathbf{x}_i)$  is an image embedding and  $y_i$  its corresponding label. By minimising this loss, distances between embeddings from the same class will be minimised, while distances between embeddings from different classes will be maximised. This bears similarities to the (supervised) contrastive loss (Khosla et al., 2020; Chen et al., 2020a), which we discuss in Appendix A.3. For ease of discussion, we refer to the distances between pairs of embeddings from the same class as *positives*, and to the distances between pairs of embeddings from different classes as *negatives*.

Importantly, the concepts of support set and query set of Sec. 3.1 and 3.2 here do not apply. More simply, the images (and respective labels) constituting the batch  $B = \{(\mathbf{x}_1, y_1), \dots, (\mathbf{x}_b, y_b)\}$  are sampled i.i.d. from the training dataset, as normally happens in standard supervised learning. Considering that in PNs there is no parameter adaptation happening at the level of each episodic batch  $B_E$ ,  $S$  and  $Q$  do not have a functional role in the algorithm, and their defining values  $\{w, m, n\}$  can be interpreted as hyperparameters controlling the data-loader during training. More specifically, PNs differ from NCA in three key aspects:

1. PNs rely on the creation of prototypes, while NCA does not.
2. Due to the nature of episodic learning, PNs only consider pairwise distances between the query and the support set; the NCA instead uses *all* the distances within a batch and treats each example in the same way.

3. Because of how  $L$ ,  $S$  and  $Q$  are sampled in episodic learning, some images will be inevitably sampled more frequently than others, and some will likely never be seen during training (this corresponds to sampling “with replacement”). NCA instead visits every image of the dataset once and only once within each epoch (sampling “without replacement”).

**Notes on data-efficiency in batch exploitation.** To expand on point 2 above, Fig. 1 illustrates the difference in batch exploitation. For PNs (*left*) and a training episode of  $w=3$  ways,  $n=3$  shots and  $m=1$  queries, the total number distances contributing to the loss consists of  $wmn = 9$  positives and  $w(w-1)mn = 18$  negatives<sup>2</sup>. If we consider the *same* training batch in a non-episodic way, when computing the NCA loss (Fig. 1 *right*) we have  $\binom{m+n}{2}w = 18$  positives and  $\binom{w}{2}(m+n)^2 = 48$  negatives (we summarise these equations in Table 1). This difference in batch exploitation is significant; in Appendix A.7 we show that it grows exponentially as  $O(w^2(m^2 + n^2))$ .

To investigate the effect of the three key differences between PNs and NCA illustrated in this section, in Sec. 4 we conduct a wide range of experiments.

### 3.4 Few-shot classification during evaluation

Once  $f_\theta$  has been trained, there are many possible ways to perform few-shot classification during evaluation. In this paper, we consider three simple approaches that are particularly aligned for embeddings learned via metric-based losses such as Eq. 2 or Eq. 3.

**$k$ -NN.** To classify an image  $\mathbf{q}_i \in Q$ , we first compute the Euclidean distance to each support point  $\mathbf{s}_j \in S$ :  $d_{ij} = \|f_\theta(\mathbf{q}_i) - f_\theta(\mathbf{s}_j)\|^2$ . Then, we simply assign  $y(\mathbf{q}_i)$  to be majority label of the  $k$  nearest neighbours. A downside here is that  $k$  is a hyperparameter that has to be chosen, although a reasonable choice in the FSL setup is to set it equal to the number of “shots”  $n$ .

**1-NN with Class Centroids.** Similar to  $k$ -NN, we can perform classification by inheriting the label of the closest class centroid, i.e.  $y(\mathbf{q}_i) = \arg \min_{j \in \{1, \dots, k\}} \|f_\theta(\mathbf{x}_i) - \mathbf{c}_j\|$ . This is the approach used at test-time by Snell et al. (2017) and Wang et al. (2019).

**Soft-assignments.** To classify an image  $\mathbf{q}_i \in Q$ , we compute the values

$$p_{ij} = \frac{\exp(-\|f_\theta(\mathbf{q}_i) - f_\theta(\mathbf{s}_j)\|^2)}{\sum_{\mathbf{s}_k \in S} \exp(-\|f_\theta(\mathbf{q}_i) - f_\theta(\mathbf{s}_k)\|^2)}$$

for all  $\mathbf{s}_j \in S$ , which is the probability that image  $i$  is sampled from image  $j$ . We then compute the likelihood for each class  $k$ :  $\sum_{\mathbf{s}_j \in S_k} p_{ij}$ , and choose the class with the highest likelihood  $y(\mathbf{q}_i) = \arg \max_k \sum_{\mathbf{s}_j \in S_k} p_{ij}$ . This is what the original NCA paper (Goldberger et al., 2005) used for evaluation, and has a direct probabilistic interpretation.

We also experimented with using the NCA loss on the support set to perform adaptation at test time, which we discuss in Appendix A.1.

## 4 Experiments

In the following, Sec. 4.1 describes our experimental setup. Sec. 4.2 shows the effect of the hyperparameters controlling the creation of episodes in PNs. In Sec. 4.3 we perform a set of ablation studies to better illustrate the relationship between PNs and the NCA. Finally, in Sec. 4.4 we compare our version of the NCA to several recent methods on three FSL benchmarks.

<sup>2</sup>The number of distances computed in the batch is actually even smaller for PNs:  $wm=3$  positives and  $w(w-1)m=6$  negatives. However, since gradients are propagated through prototypes, the distances to the individual support points can be considered as contributing to the loss. This is what we do throughout the paper.

<i>miniImageNet</i>		
method	5-shot val	5-shot test
<i>Soft-assignment</i>	79.11 $\pm$ 0.27	77.16 $\pm$ 0.10
<i>k</i> -NN	75.82 $\pm$ 0.21	73.52 $\pm$ 0.12
1-NN centroid	<b>80.61 <math>\pm</math> 0.20</b>	<b>78.30 <math>\pm</math> 0.14</b>
CIFAR-FS		
<i>Soft-assignment</i>	76.12 $\pm$ 0.32	83.31 $\pm$ 0.37
<i>k</i> -NN	73.46 $\pm$ 0.39	80.94 $\pm$ 0.38
1-NN centroid	<b>77.80 <math>\pm</math> 0.35</b>	<b>85.13 <math>\pm</math> 0.32</b>

Table 2: Comparison between the different test-time strategies discussed in Sec. 3.4.

## 4.1 Experimental setup

We conduct our experiments on *miniImageNet* (Vinyals et al., 2016), CIFAR-FS (Bertinetto et al., 2019) and *tieredImageNet* (Ren et al., 2018), using the ResNet12 variant first adopted by Lee et al. (2019) as embedding function  $f_\theta$ . A detailed description of benchmarks, architecture and implementation details is deferred to Appendix A.4, while below we discuss the most important choices.

Like Wang et al. (2019), for all our experiments (including those with Prototypical and Matching Networks) we centre and normalise the feature embeddings before performing classification, as it is considerably beneficial for performance. After training, we compute the mean feature vectors of all the images in the training set:  $\bar{\mathbf{x}} = \frac{1}{|\mathcal{D}^{\text{train}}|} \sum_{\mathbf{x} \in \mathcal{D}^{\text{train}}} \mathbf{x}$ . Then, all feature vectors in the test set are updated as  $\mathbf{x}_i \leftarrow \mathbf{x}_i - \bar{\mathbf{x}}$ , and normalised by  $\mathbf{x}_i \leftarrow \frac{\mathbf{x}_i}{\|\mathbf{x}_i\|}$ .

We compared the inference methods discussed in Sec. 3.4 on *miniImageNet* and CIFAR-FS. Results can be found in Table 2. Unless expressly specified, we chose to use 1-NN with class centroids in all our experiments, as it performs significantly better than *k*-NN or *Soft-assignment*. This might sound surprising, as the *Soft-assignment* approach closely reflects NCA’s training protocol and outputs class probabilities. We speculate its inferior performance could be caused by poor model calibration (Guo et al., 2017): since the classes between training and evaluation are disjoint, the model is unlikely to produce calibrated probabilities. As such, within the softmax, outliers behaving as false positives can happen to highly influence the final decision, and those behaving as false negatives can end up being almost completely ignored (their contribution is squashed toward zero). With the nearest centroid classification approach outliers are still clearly an issue, but their effect can be less dramatic.

As standard, performance is assessed on episodes of 5-way, 15-query and either 1- or 5-shot. Each model is evaluated on 10,000 episodes sampled from the test set (or the validation set, in some experiments). To further reduce the variance, we trained each model *five times* with five different random seeds, for a total of 50,000 episodes per configuration, from which 95% confidence intervals are computed and reported for all our experiments.

## 4.2 Considerations on episodes and data efficiency

Despite Prototypical Networks being one of the simplest FSL methods, the creation of episodes requires the use of several hyperparameters ( $\{w, m, n\}$ , Sec. 3.1) which can significantly affect performance. Snell et al. (2017) state that the number of shots  $n$  between training and testing should match and that one should use a higher number of ways  $w$  during training time. In their experiments, they train 1-shot models with  $w = 30$ ,  $n = 1$ ,  $m = 15$  and 5-shot models with  $w = 20$ ,  $n = 5$ ,  $m = 15$ . This makes the corresponding batch sizes of these episodes 480 and 400, respectively. Since, as seen in Sec. 3.3, the number of positives and negatives grows rapidly for both PNs and NCA (although at a different rate), this makes a fair comparison between models trained on different types of episodes difficult.

We investigate the effect of changing these hyperparameters in a systematic manner. To compare configurations fairly across episode/batch sizes, we define each configuration by its number of shots  $n$ , the batch size  $b$  and the total number of images per class  $a$  (which accounts for the sum between support

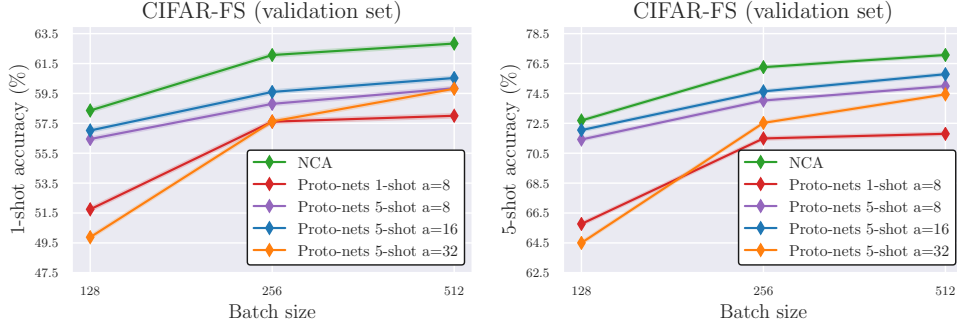


Figure 2: 1-shot and 5-shot accuracies on the validation set of CIFAR-FS. Models trained using NCA or Prototypical Networks loss with different configurations: 1-shot with  $a=8$  and 5-shot with  $a=8$ , 16 or 32. Values correspond to the mean accuracy of five models trained with different random seeds. Please see Sec. 4.2 for details.

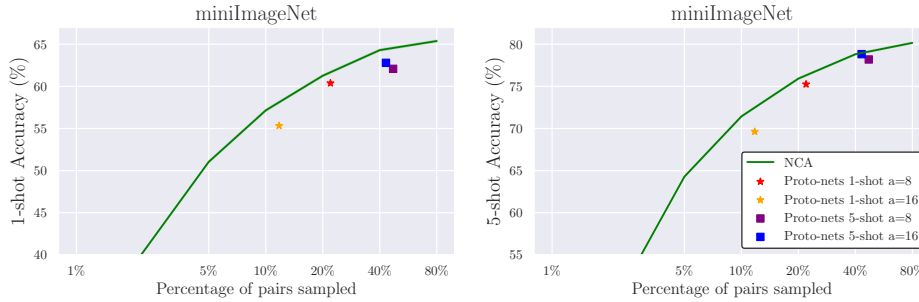


Figure 3: 1-shot and 5-shot accuracies on the validation set of *miniImageNet* for NCA models trained by only sampling a fraction of the total number of available pairs in the batch (of size 256). Stars and squares represent models trained using PNs, and are plotted on the x-axis based on the total number of distance pairs exploited in the loss, so that they can be directly compared with this “sub-sampling” variant of the NCA. Reported values correspond to the mean accuracy of five models trained with different random seeds. Please see Sec. 4.2 for details.

and query set,  $a = n + m$ ). For example, if we train a 5-shot model with  $a = 8$  and  $b = 256$ , it means that its corresponding training episodes will have  $n = 5$ ,  $q = 8 - 5 = 3$ , and  $w = 256/8 = 32$ . Using this notation, we train configurations of PNs covering several combinations of these hyperparameters so that the resulting batch size corresponding to an episode is 128, 256 or 512. Then, we train three configurations of NCA, where the only hyperparameter is the batch size.

Results for CIFAR-FS can be found in Fig. 2, where we report results for NCA and PNs with  $a = 8$ , 16 or 32. Results for *miniImageNet* observe the same trend and are deferred to Appendix A.6. Note that PNs’ results for 1-shot with  $a = 16$  and  $a = 32$  are *not reported*, as they fare significantly worse. Several things can be noticed. First, NCA performs better than *all* PNs configurations, no matter the batch size. Second, PNs are very sensitive to different hyperparameter configurations. For instance, with batches of size 128, PNs trained with episodes of 5-shot and  $a = 32$  perform significantly worse than a PNs trained with episodes of 5-shot and  $a = 16$ . Finally, we can also notice that, contrary to what has been previously reported (Snell et al., 2017; Cao et al., 2020), the 5-shot model with the best configuration is always strictly better than any 1-shot configuration. We speculate that this is probably due to the fact that we compare configurations keeping the batch size constant.

**Episodic batches vs random sub-sampling of standard batches.** Despite NCA outperforming all PNs configurations (Fig. 2), one might posit that by using more distances within a batch, NCA is more computationally costly and thus the episodic strategy of PNs can sometimes be advantageous (e.g. real-time applications with large batches). To investigate this, we perform an experiment where we train NCA models by randomly sampling a fraction of the total number of distances used in the loss. Then, for comparison, we include different PNs models after having computed to which percentage of discarded pairs (in a normal batch) their episodic batch corresponds to.



Figure 4: Ablation experiments on NCA and Prototypical Networks, both on batches (or episodes) of size 128, 256, and 512 on the validation sets of *miniImageNet* and CIFAR-FS. Please refer to Sec. 4.3 for details.

Results can be found in Fig. 3. As expected, we can see how sub-sampling a fraction of the total available number of pairs within a batch negatively affects performance. To answer to possible concerns on computational efficiency, we can notice that the PN’s points lie very close to the under-sampling version of the NCA, which signals that the episodic strategy of PN’s is roughly equivalent to training with the NCA and to only exploiting a fraction of the distances available in a batch.

Note how, moving along the x-axis of Fig. 3, variants of PN’s exploiting a higher number of distances perform better. In Appendix A.8 we look more carefully whether the difference in performance between the different episodic batch setups of Fig. 2 can be solely explained by the differences in the number of distance pairs used in the batch configurations. We indeed find that generally speaking the higher the number of pairs the better, however, one should also consider the positive/negative balance and the number of classes present within a batch.

### 4.3 Ablation experiments

To better analyse why NCA performs better than PN’s, in this section we consider the three key differences discussed earlier by performing a series of ablations on models trained on batches of size 128, 256 and 512. Results are summarised in Fig. 4. We refer the reader to Appendix A.1 to obtain detailed steps describing how these ablations affect Eq. 2 and Eq. 3.

First, we compare two variants of NCA: one in which the sampling of the training batches happens sequentially and without replacement, as it is standard in supervised learning, and one where the batches are sampled with replacement. Interestingly, this modification (row 1 and 2 of Fig. 4) has a negligible effect across the two datasets and four splits considered, meaning that the replacement sampling introduced by episodic learning will not interfere with the other ablations.

We then perform a series of ablations on episodic batches, i.e. sampled with the method described in Sec. 3.1. For PN’s ablations, we perform experiments on 1-shot and 5-shot models with  $a = 8$ . This means that PN’s models are trained with 8 images per class, and either 16, 32 or 64 classes for the batch sizes 128, 256 and 512 respectively. The batch size for the NCA is also set to either 128, 256, or 512, allowing a fair comparison.

First, we train standard PN’s models (row 4 and 5 of Fig. 4). Next, we train a PN’s model where “prototypes” are not computed (point 1 of Sec. 3.3), meaning that distances are considered between individual points, but a separation between query and support set remains (row 6). Then, we perform an ablation where we ignore the separation between support and query set (point 2 of Sec. 3.3), and compute the NCA on the union of the support and query set, while still computing prototypes for the points that would belong to the support set (last row). Last, we perform an ablation where we consider all the previous points together: we sample with replacement, we ignore the separation between support and query set and we do not compute prototypes. This amounts to the NCA loss, except that it is computed on batches with a fixed number of classes and a fixed number of images per class (row 3).

Notice that in Fig. 4 there is only one row dedicated to 1-shot models. This is because we cannot generate prototypes from 1-shot models, so we cannot have a “no proto” ablation. Furthermore, for





Figure 5: Ablation experiments on NCA and Matching Networks, both on batches (or episodes) of size 128, 256 and 512 on the validation sets of *miniImageNet* and CIFAR-FS. All methods use the *Soft-assignment* strategy (Sec. 3.4) for evaluation.

1-shot models the “no S/Q” ablation is equivalent to the NCA with a fixed batch composition.

From Fig. 4, we can see that disabling prototypes (row 6) negatively affects the performance of 5-shot (row 5), albeit slightly. On the other hand, enabling the computation between all pairs increases the performance (last row). Importantly, enabling all the ablations (row 3) completely recovers the performance lost by PNs.

Notice the meaningful gap in performance between row 1 and 3 in Fig. 4 for batch size 128, which disappears for batch size 512. This is likely due to the number of positives available in an excessively small batch size. Since our vanilla NCA relies on using distance pairs and creates batches by simply sampling images randomly from the dataset, there is a limit to how small a batch can be (which depends on the number of classes of the dataset). As an example, consider the extreme case of a batch of size 4. For the datasets considered, it is very likely that such a batch will contain no positive pairs for some classes. For a batch size of 128 and a training set of 64 classes, with a parameter-free sampler the NCA will have in expectation only one positive pair per class. Conversely, the NCA ablation with a fixed batch composition (i.e. with a set number of images per class) will have a higher number of positive pairs (at the cost of a reduced number of classes per batch). This can explain the difference, as positive pairs constitute a less frequent (and potentially more informative) training signal. For the sake of simplicity, and since this only affects smaller batch sizes, we opted to use a vanilla, parameter-free sampler for the NCA in the rest of our experiments.

The fact that every single ablation does not have much influence on the performance, but their combination does, could be explained by the number of distance pairs exploited by the individual ablations. Using the formulas described at the end of Section 3.3, we compute the number of positives and negatives used for each ablation. For row 6 there are 480 positives and 14,880 negatives. For row 7 there are 576 positives and 20,170 negatives. In both cases, the number is significantly lower than the corresponding NCA, which gets 896 positives and 31,744 negatives, and this could explain the gap between row 6 (and 7) and row 3. Moreover, from row 5 (and 6) to row 7 we see a modest increase in performance, which can also be explained by the slightly larger number of distance pairs.

These experiments highlight that the separation of roles between the images belonging to support and query set, which is typical of episodic learning (Vinyals et al., 2016), is detrimental for the performance of Prototypical Networks. Instead, using the NCA loss on standard mini-batches allows full exploitation of the training data and significantly improves performance. Moreover, the NCA has the advantage of simplifying the overall training procedure, as the hyperparameters for the creation of episodes  $\{w, n, m\}$  no longer need to be considered.

**Matching Networks (Vinyals et al., 2016) (MNs)** are closely related to PNs (Snell et al., 2017) in the multi-shot case and equivalent in the 1-shot case. The difference in the multi-shot case is in the way the support set is used. Whereas PNs generate prototypes by averaging the embeddings of the support set, MNs adopt a weighted nearest-neighbour approach using an attention mechanism, which

	miniImageNet		CIFAR-FS	
	1-shot	5-shot	1-shot	5-shot
<b>Episodic methods</b>				
adaResNet (Munkhdalai et al., 2018)	56.88 $\pm$ 0.62	71.94 $\pm$ 0.57	-	-
TADAM(Oreshkin et al., 2018)	58.50 $\pm$ 0.30	76.70 $\pm$ 0.30	-	-
Shot-Free (Ravichandran et al., 2019)	60.71 $\pm$ n/a	77.64 $\pm$ n/a	69.2 $\pm$ n/a	84.7 $\pm$ n/a
TEAM (Qiao et al., 2019)	60.07 $\pm$ n/a	75.90 $\pm$ n/a	-	-
MTL (Sun et al., 2019)	61.20 $\pm$ 1.80	75.50 $\pm$ 0.80	-	-
TapNet (Yoon et al., 2019)	61.65 $\pm$ 0.15	76.36 $\pm$ 0.10	-	-
MetaOptNet-SVM(Lee et al., 2019)	62.64 $\pm$ 0.61	78.63 $\pm$ 0.46	<b>72.0 <math>\pm</math> 0.7</b>	84.2 $\pm$ 0.5
Variational FSL (Zhang et al., 2019)	61.23 $\pm$ 0.26	77.69 $\pm$ 0.17	-	-
<b>Simple baselines</b>				
Transductive finetuning (Dhillon et al., 2020)	62.35 $\pm$ 0.66	74.53 $\pm$ 0.54	70.76 $\pm$ 0.74	81.56 $\pm$ 0.53
RFIC-simple (Tian et al., 2020)	62.02 $\pm$ 0.63	<b>79.64 <math>\pm</math> 0.44</b>	71.5 $\pm$ 0.8	86.0 $\pm$ 0.5
Meta-Baseline (Chen et al., 2020b)	<b>63.17 <math>\pm</math> 0.23</b>	79.26 $\pm$ 0.17	-	-
<i>Our implementations:</i>				
Proto-nets (Snell et al. (2017) setup)	59.78 $\pm$ 0.12	75.42 $\pm$ 0.09	69.94 $\pm$ 0.12	84.01 $\pm$ 0.09
Proto-nets (our setup)	61.32 $\pm$ 0.12	77.77 $\pm$ 0.09	70.41 $\pm$ 0.12	84.61 $\pm$ 0.10
SimpleShot (Wang et al., 2019)	62.16 $\pm$ 0.12	78.33 $\pm$ 0.09	69.98 $\pm$ 0.12	84.40 $\pm$ 0.09
<b>NCA (ours)</b>	62.55 $\pm$ 0.12	78.27 $\pm$ 0.09	<b>72.49 <math>\pm</math> 0.12</b>	<b>85.15 <math>\pm</math> 0.09</b>

Table 3: Comparison with methods that use ResNet12 on *miniImageNet* and CIFAR-FS (test set).

in its simplest form corresponds to a softmax over the distances (Vinyals et al., 2016, Sec.2.1.1). This corresponds to the *Soft-assignment* approach discussed in Sec. 3.4.

Given the similarity between the two algorithms, and because of the importance both have in the FSL community, we performed analogous experiments to those of Fig. 4 for Matching Networks. The results can be found in Figure 5. In particular, we perform experiments on the simplest variant of Matching Networks described in Vinyals et al. (2016), with the softmax attention mechanism and without the Full Context Embedding. Different to Vinyals et al. (2016), we use the Euclidean distance (as opposed to the cosine distance), as it has proven to be beneficial for FSL performance by Snell et al. (2017). Given that hyperparameters for the training episodes are not specified in the original MNs paper, we adopted the same used for PNs, which we observed working well also for MNs.

The only difference between Matching Networks and NCA during training is the separation between support and query set, leaving us with only one ablation to perform. At test time, evaluating Matching Networks is equivalent to using the *Soft-assignment* approach described in Sec. 3.4. Therefore, in this experiment, for both NCA and “NCA fixed-batch composition” methods we also use the *Soft-assignment* evaluation.

As we can see, disregarding the separation between support and query set also improves the performance of Matching Networks, and significantly so. This corroborates the findings of Sec. 4.3. The separation of roles between images in the support and query sets, typical of episodic learning, is detrimental to the performance of both Prototypical and Matching Networks. Instead, using the (closely related) NCA on standard mini-batches allows for better exploitation of the training data, while simultaneously simplifying the training procedure.

#### 4.4 Comparison with the state-of-the-art

We now evaluate our models on three standard FSL datasets, with the purpose of contextualising their performance against the modern literature.

When considering which methods to compare against, we chose those *a)* that have been recently published, *b)* that are using a ResNet12 (which we found the most commonly used) and *c)* with a setup that is not significantly more complicated than ours. For example, we only report the results of the main approach proposed by Tian et al. (2020) and not their *sequential self-distillation* (Furlanello et al., 2018) variant, which requires re-training multiple times and can be applied to most methods.

Results can be found in Table 3 for *miniImageNet* and CIFAR-FS and Table 4 for *tieredImageNet*. In Table 3 we report Prototypical Networks results for both the episodic setup from Snell et al. (2017)

<i>tieredImageNet</i>		
Method	1-shot	5-shot
Shot-Free (Ravichandran et al., 2019)	63.52 $\pm$ n/a	82.59 $\pm$ n/a
RFIC-simple (Tian et al., 2020)	<b>69.74 <math>\pm</math> 0.72</b>	<b>84.41 <math>\pm</math> 0.55</b>
Meta-Baseline (Chen et al., 2020b)	68.62 $\pm$ 0.27	83.29 $\pm$ 0.18
MetaOptNet-SVM(Lee et al., 2019)	65.99 $\pm$ 0.72	81.56 $\pm$ 0.53
<i>Our implementations:</i>		
Proto-nets (Snell et al. (2017) setup)	65.80 $\pm$ 0.13	81.26 $\pm$ 0.10
SimpleShot (Wang et al., 2019)	66.67 $\pm$ 0.14	81.57 $\pm$ 0.10
<b>NCA (ours)</b>	68.35 $\pm$ 0.13	83.20 $\pm$ 0.10

Table 4: Comparison with methods that use ResNet12 on *tieredImageNet* (test set).

and the best one (batch size 512, 5-shot,  $a=16$ ) found from the experiment of Fig. 2, which brings a considerable improvement over the original. We did not optimise for a new setup for Prototypical Networks on *tieredImageNet*, as the larger dataset and the higher number of classes would have made the hyperparameter search too demanding. Notice how our vanilla NCA is competitive and sometimes even superior to recent methods, despite being extremely simple. It fairs surprisingly well against methods that use meta-learning (and episodic learning), and also against the high-performing simple baselines based on pre-training with the cross-entropy loss.

## 5 Conclusion

Towards the aim of understanding the reasons behind the poor competitiveness of meta-learning methods with respect to simple baselines, in this paper we start by investigating the role of episodes in the popular Prototypical Networks. We found that their performance is highly sensitive to the set of hyperparameters used to sample the episodes. By replacing Prototypical Networks loss with the classic Neighbourhood Component Analysis, we are able to ignore these hyperparameters while significantly improving the few-shot classification accuracy. With a series of experiments, we found out that the performance discrepancy mostly arises from the separation between support and query set within each episode, and that Prototypical Networks’ episodic strategy is almost empirically equivalent to randomly discarding a large fraction of distances within a standard mini-batch. Finally, we show that our variant of the NCA achieves an accuracy on multiple popular FSL benchmarks that is comparable or superior with state-of-the-art methods of similar complexity, making it a simple and appealing baseline for future work.

## References

- Kelsey R Allen, Evan Shelhamer, Hanul Shin, and Joshua B Tenenbaum. Infinite mixture prototypes for few-shot learning. In *International Conference on Machine Learning*, 2019.
- Han Altae-Tran, Bharath Ramsundar, Aneesh S Pappu, and Vijay Pande. Low data drug discovery with one-shot learning. *ACS central science*, 2017.
- Samy Bengio, Yoshua Bengio, Jocelyn Cloutier, and Jan Gecsei. On the optimization of a synaptic learning rule. In *Preprints Conf. Optimality in Artificial and Biological Neural Networks*. Univ. of Texas, 1992.
- Luca Bertinetto, João F Henriques, Jack Valmadre, Philip Torr, and Andrea Vedaldi. Learning feed-forward one-shot learners. In *Advances in Neural Information Processing Systems*, 2016.
- Luca Bertinetto, João F Henriques, Philip HS Torr, and Andrea Vedaldi. Meta-learning with differentiable closed-form solvers. In *International Conference on Learning Representations*, 2019.

- Qi Cai, Yingwei Pan, Ting Yao, Chenggang Yan, and Tao Mei. Memory matching networks for one-shot image recognition. In *Proceedings of the IEEE Conference on Computer Vision and Pattern Recognition (CVPR)*, June 2018.
- Tianshi Cao, Marc Law, and Sanja Fidler. A theoretical analysis of the number of shots in few-shot learning. In *International Conference on Learning Representations*, 2020.
- Ting Chen, Simon Kornblith, Mohammad Norouzi, and Geoffrey Hinton. A simple framework for contrastive learning of visual representations. *arXiv preprint arXiv:2002.05709*, 2020a.
- Wei-Yu Chen, Yen-Cheng Liu, Zsolt Kira, Yu-Chiang Frank Wang, and Jia-Bin Huang. A closer look at few-shot classification. *arXiv preprint arXiv:1904.04232*, 2019.
- Yinbo Chen, Xiaolong Wang, Zhuang Liu, Huijuan Xu, and Trevor Darrell. A new meta-baseline for few-shot learning. *arXiv preprint arXiv:2003.04390*, 2020b.
- Tristan Deleu, Tobias Würfl, Mandana Samiei, Joseph Paul Cohen, and Yoshua Bengio. Torchmeta: A meta-learning library for pytorch. *arXiv preprint arXiv:1909.06576*, 2019.
- Guneet S Dhillon, Pratik Chaudhari, Avinash Ravichandran, and Stefano Soatto. A baseline for few-shot image classification. In *International Conference on Learning Representations*, 2020.
- Chelsea Finn, Pieter Abbeel, and Sergey Levine. Model-agnostic meta-learning for fast adaptation of deep networks. In *International Conference on Machine Learning*, 2017.
- Tommaso Furlanello, Zachary Lipton, Michael Tschannen, Laurent Itti, and Anima Anandkumar. Born again neural networks. In *International Conference on Machine Learning*, 2018.
- Golnaz Ghiasi, Tsung-Yi Lin, and Quoc V Le. Dropblock: A regularization method for convolutional networks. In *Advances in Neural Information Processing Systems*, 2018.
- Spyros Gidaris, Andrei Bursuc, Nikos Komodakis, Patrick Pérez, and Matthieu Cord. Boosting few-shot visual learning with self-supervision. In *IEEE Conference on Computer Vision and Pattern Recognition*, 2019.
- Jacob Goldberger, Geoffrey E Hinton, Sam T Roweis, and Russ R Salakhutdinov. Neighbourhood components analysis. In *Advances in Neural Information Processing Systems*, 2005.
- Alex Graves, Greg Wayne, and Ivo Danihelka. Neural turing machines. *arXiv preprint arXiv:1410.5401*, 2014.
- Edward Grefenstette, Brandon Amos, Denis Yarats, Phu Mon Htut, Artem Molchanov, Franziska Meier, Douwe Kiela, Kyunghyun Cho, and Soumith Chintala. Generalized inner loop meta-learning. *arXiv preprint arXiv:1910.01727*, 2019.
- Chuan Guo, Geoff Pleiss, Yu Sun, and Kilian q Weinberger. On calibration of modern neural networks. In *International Conference on Machine Learning*, 2017.
- Timothy Hospedales, Antreas Antoniou, Paul Micaelli, and Amos Storkey. Meta-learning in neural networks: A survey. *arXiv preprint arXiv:2004.05439*, 2020.
- Prannay Khosla, Piotr Teterwak, Chen Wang, Aaron Sarna, Yonglong Tian, Phillip Isola, Aaron Maschinot, Ce Liu, and Dilip Krishnan. Supervised contrastive learning. *arXiv preprint arXiv:2004.11362*, 2020.
- Brenden M Lake, Ruslan Salakhutdinov, and Joshua B Tenenbaum. Human-level concept learning through probabilistic program induction. *Science*, 2015.

- Kwonjoon Lee, Subhansu Maji, Avinash Ravichandran, and Stefano Soatto. Meta-learning with differentiable convex optimization. In *IEEE Conference on Computer Vision and Pattern Recognition*, 2019.
- George A Miller. Wordnet: a lexical database for english. *Communications of the ACM*, 38(11):39–41, 1995.
- Tsendsuren Munkhdalai, Xingdi Yuan, Soroush Mehri, and Adam Trischler. Rapid adaptation with conditionally shifted neurons. In *International Conference on Machine Learning*, 2018.
- Boris Oreshkin, Pau Rodríguez López, and Alexandre Lacoste. Tadam: Task dependent adaptive metric for improved few-shot learning. In *Advances in Neural Information Processing Systems*, 2018.
- Hang Qi, Matthew Brown, and David G Lowe. Low-shot learning with imprinted weights. In *IEEE Conference on Computer Vision and Pattern Recognition*, 2018.
- Limeng Qiao, Yemin Shi, Jia Li, Yaowei Wang, Tiejun Huang, and Yonghong Tian. Transductive episodic-wise adaptive metric for few-shot learning. In *IEEE International Conference on Computer Vision*, 2019.
- Aniruddh Raghu, Maithra Raghu, Samy Bengio, and Oriol Vinyals. Rapid learning or feature reuse? towards understanding the effectiveness of maml. In *International Conference on Learning Representations*, 2020.
- Sachin Ravi and Hugo Larochelle. Optimization as a model for few-shot learning. In *International Conference on Learning Representations*, 2017.
- Avinash Ravichandran, Rahul Bhotika, and Stefano Soatto. Few-shot learning with embedded class models and shot-free meta training. In *IEEE International Conference on Computer Vision*, 2019.
- Mengye Ren, Eleni Triantafillou, Sachin Ravi, Jake Snell, Kevin Swersky, Joshua B Tenenbaum, Hugo Larochelle, and Richard S Zemel. Meta-learning for semi-supervised few-shot classification. In *International Conference on Learning Representations*, 2018.
- Ruslan Salakhutdinov and Geoff Hinton. Learning a nonlinear embedding by preserving class neighbourhood structure. In *Artificial Intelligence and Statistics*, 2007.
- Adam Santoro, Sergey Bartunov, Matthew Botvinick, Daan Wierstra, and Timothy Lillicrap. Meta-learning with memory-augmented neural networks. In *International Conference on Machine Learning*, 2016.
- Jürgen Schmidhuber. *Evolutionary principles in self-referential learning, or on learning how to learn: the meta-meta-... hook*. PhD thesis, Technische Universität München, 1987.
- Jürgen Schmidhuber. Learning to control fast-weight memories: An alternative to dynamic recurrent networks. *Neural Computation*, 1992.
- Jake Snell, Kevin Swersky, and Richard Zemel. Prototypical networks for few-shot learning. In *Advances in Neural Information Processing Systems*, 2017.
- Qianru Sun, Yaoyao Liu, Tat-Seng Chua, and Bernt Schiele. Meta-transfer learning for few-shot learning. In *IEEE Conference on Computer Vision and Pattern Recognition*, 2019.
- Sebastian Thrun. Is learning the n-th thing any easier than learning the first? In *Advances in Neural Information Processing Systems*, 1996.
- Yonglong Tian, Yue Wang, Dilip Krishnan, Joshua B Tenenbaum, and Phillip Isola. Rethinking few-shot image classification: a good embedding is all you need? *arXiv preprint arXiv:2003.11539*, 2020.

- Eleni Triantafillou, Tyler Zhu, Vincent Dumoulin, Pascal Lamblin, Utku Evci, Kelvin Xu, Ross Goroshin, Carles Gelada, Kevin Swersky, Pierre-Antoine Manzagol, et al. Meta-dataset: A dataset of datasets for learning to learn from few examples. In *International Conference on Learning Representations*, 2019.
- Paul E Utgoff. Shift of bias for inductive concept learning. *Machine learning: An artificial intelligence approach*, 1986.
- Ricardo Vilalta and Youssef Drissi. A perspective view and survey of meta-learning. *Artificial Intelligence Review*, 2002.
- Oriol Vinyals, Charles Blundell, Timothy Lillicrap, Daan Wierstra, et al. Matching networks for one shot learning. In *Advances in Neural Information Processing Systems*, 2016.
- Yan Wang, Wei-Lun Chao, Kilian Q Weinberger, and Laurens van der Maaten. Simpleshot: Revisiting nearest-neighbor classification for few-shot learning. *arXiv preprint arXiv:1911.04623*, 2019.
- Sung Whan Yoon, Jun Seo, and Jaekyun Moon. Tapnet: Neural network augmented with task-adaptive projection for few-shot learning. In *International Conference on Machine Learning*, 2019.
- Jian Zhang, Chenglong Zhao, Bingbing Ni, Minghao Xu, and Xiaokang Yang. Variational few-shot learning. In *IEEE International Conference on Computer Vision*, 2019.

## A Appendix

### A.1 Performance improvements

**Adapting to the support set.** Prototypical Networks does not perform any kind of parameter adaptation at test time. On the one hand this is convenient, as it allows fast inference; on the other hand, useful information from the support set  $S$  might remain unexploited.

In the 5-shot case it is possible to minimise the NCA loss since it can directly be computed on the support set:  $\mathcal{L}_{\text{NCA}}(S)$ . We tried training a positive semi-definite matrix  $A$  on the outputs of the trained neural network, which corresponds to learning a Mahalanobis distance metric as in Goldberger et al. (2005). However, we found that there was no meaningful increase in performance. Differently, we did find that fine-tuning the entire network  $f_\theta$  via the optimisation of  $\arg \min_\theta \mathcal{L}_{\text{NCA}}(S)$  was beneficial (see Table 5). However, given the computational cost, we opted for not performing adaptation to the support set in the experiments of Sec. 4.

**Features concatenation.** For NCA, we also found that concatenating the output of intermediate layers modestly improves performance at (almost) no additional cost. We used the output of the average pool layers from all ResNet blocks except the first and we refer to this variant as NCA multi-layer. However, since this is an orthogonal variation that can be applied to several methods, we do not consider it for our experiments of Sec. 4.

Results on *miniImageNet* and CIFAR-FS are shown in Table 5.

### A.2 Details about the ablation studies of Section 4.3

Referring to the three key differences between the loss of Prototypical Networks and the NCA loss listed in Sec. 3.3, in this section we detail how to obtain the ablations we used to perform the experiments of Sec. 4.3.

We can “disable” the creation of prototypes (*point 1* of Sec. 3.3), which will change the prototypical loss of Eq. 2 to

$$\mathcal{L}(S, Q) = -\frac{1}{|Q| + |S|} \sum_{(\mathbf{q}_i, y) \in Q} \log \left( \frac{\sum_{(\mathbf{s}_j, y') \in S_y} \exp -\|\mathbf{q}_i - \mathbf{s}_j\|^2}{\sum_{(\mathbf{s}_k, y'') \in S} \exp -\|\mathbf{q}_i - \mathbf{s}_k\|^2} \right). \quad (4)$$

This is similar to  $\mathcal{L}_{\text{NCA}}$  (Eq. 3), where the positives are represented by the distances from  $Q$  to  $S_k$ , and the negatives by the distances from  $Q$  to  $S \setminus S_k$ . The only difference now is the separation of the batch into a query and support set.

Independently, we can “disable” *point 2* of Sec. 3.3, which gives us

$$\mathcal{L}(S, Q) = -\frac{1}{|Q| + |S|} \sum_{(\mathbf{z}_i, y_i) \in Q \cup C} \log \left( \frac{\sum_{\substack{(\mathbf{z}_j, y_j) \in Q \cup C \\ y_j = y_i \\ i \neq j}} \exp -\|\mathbf{z}_i - \mathbf{z}_j\|^2}{\sum_{\substack{(\mathbf{z}_k, y_k) \in Q \cup C \\ k \neq i}} \exp -\|\mathbf{z}_i - \mathbf{z}_k\|^2} \right), \quad (5)$$

which essentially combines the prototypes with the query set, and computes the NCA loss on that total set of embeddings.

Finally, we can “disable” both point 1 and 2, which gives us

$$\mathcal{L}(S, Q) = -\frac{1}{|Q| + |S|} \sum_{(\mathbf{z}_i, y_i) \in Q \cup S} \log \left( \frac{\sum_{\substack{(\mathbf{z}_j, y_j) \in Q \cup S \\ y_j = y_i \\ i \neq j}} \exp -\|\mathbf{z}_i - \mathbf{z}_j\|^2}{\sum_{\substack{(\mathbf{z}_k, y_k) \in Q \cup S \\ k \neq i}} \exp -\|\mathbf{z}_i - \mathbf{z}_k\|^2} \right). \quad (6)$$

method	miniImageNet		CIFAR-FS	
	1-shot	5-shot	1-shot	5-shot
NCA	$62.52 \pm 0.24$	$78.3 \pm 0.14$	$72.48 \pm 0.40$	$85.13 \pm 0.29$
NCA +MULTI-LAYER	$63.21 \pm 0.08$	$79.27 \pm 0.08$	$72.44 \pm 0.36$	$85.42 \pm 0.29$
NCA +MULTI-LAYER + SS	-	<b><math>79.79 \pm 0.08</math></b>	-	<b><math>85.66 \pm 0.32</math></b>

Table 5: Comparison between vanilla NCA, NCA using features from multiple layers, and NCA performing optimisation on the support set (ss). The NCA can only be optimised in the 5-shot case, since there are not enough positives distances in the 1-shot case. Optimisation is conducted for 5 epochs using Adam, with learning rate 0.0001 and weight decay 0.0005. For details, see Sec. A.1

This almost exactly corresponds to the NCA loss, where the only difference is the construction of batches with a fixed number of classes and a fixed number of images per class.

### A.3 Differences between the NCA and contrastive losses

Eq. 3 is similar to the contrastive loss functions (Khosla et al., 2020; Chen et al., 2020a) that are used in self-supervised learning and representation learning. The main differences are that *a*) in contrastive losses, the denominator only contains negative pairs and *b*) the inner sum in the numerator is moved outside of the logarithm in the supervised contrastive loss function from Khosla et al. (2020). We opted to work with the NCA loss because we found it performs better than the supervised contrastive loss in a few-shot learning setting. Using the supervised contrastive loss we only managed to obtain 51.05% 1-shot and 63.36% 5-shot performance on the *miniImageNet* test set.

### A.4 Implementation details

**Benchmarks.** In our experiments, we use three popular FSL benchmarks. *miniImageNet* (Vinyals et al., 2016) is a subset of ImageNet generated by randomly sampling 100 classes, each with 600 randomly sampled images. We adopt the commonly used splits of Ravi & Larochelle (2017) who use 64 classes for meta-training, 16 for meta-validation and 20 for meta-testing. *CIFAR-FS* was proposed by Bertinetto et al. (2019) as an analogous version of *miniImageNet* for CIFAR-100. It uses the same sized splits and same number of images per split as *miniImageNet*. *tieredImageNet* (Ren et al., 2018) is also constructed from ImageNet, but contains 608 classes, with 351 training classes, 97 validation classes and 160 test classes. Its class splits have been generated using WordNet (Miller, 1995) to ensure that the training classes are semantically “distant” to the validation and test classes. For all datasets, we use images of size  $84 \times 84$ .

**Architecture.** In all our experiments,  $f_\theta$  is represented by a ResNet12 with “widths” [64, 160, 320, 640]. We chose this architecture, first adopted by Lee et al. (2019), as it is the one which is most frequently featured in recent FSL methods. Unlike most methods, we do not use a DropBlock regulariser (Ghiasi et al., 2018), as we did not notice it to meaningfully contribute to performance.

**Optimisation.** To train all the models used for our experiments, unless differently specified, we used a SGD optimiser with Nesterov momentum, weight decay of 0.0005 and initial learning rate of 0.1. For *miniImageNet* and *CIFAR-FS* we decrease the learning rate by a factor of 10 after 70% of epochs have been trained, and train for a total of 120 epochs. As data augmentations, we use random horizontal flipping and centre cropping.

Only for the experiments of Sec. 4.4, we slightly change our training setup. On *CIFAR-FS*, we increase the number of training epochs from 120 to 240, which improved the accuracy of about 0.5%. For *tieredImageNet*, we train for 120 epochs and decrease the learning rate by a factor of 10 after 50% and 75% of the training progress. For *tieredImageNet* only we increased the batch size to 1024, and train on 64 classes and 16 images per class within a batch, as we found it beneficial. For the other datasets, it did not make a difference. This is likely due to the large number of classes of *tieredImageNet*, where



	<i>miniImageNet</i>		CIFAR-FS	
method	1-shot	5-shot	1-shot	5-shot
<b>PNs (SimpleShot)</b>	57.99 $\pm$ 0.21	74.33 $\pm$ 0.16	53.76 $\pm$ 0.22	68.54 $\pm$ 0.19
<b>PNs (ours)</b>	62.79 $\pm$ 0.12	78.82 $\pm$ 0.09	59.60 $\pm$ 0.13	74.64 $\pm$ 0.11
<b>NCA (SimpleShot)</b>	61.21 $\pm$ 0.22	76.39 $\pm$ 0.16	59.41 $\pm$ 0.24	73.29 $\pm$ 0.19
<b>NCA (ours)</b>	64.94 $\pm$ 0.13	80.12 $\pm$ 0.09	62.07 $\pm$ 0.14	76.26 $\pm$ 0.10

Table 6: Comparison (on the validation set of *miniImageNet* and CIFAR-FS) between using the hyperparameters from SimpleShot (Wang et al., 2019) and the ones from this paper (**ours**). Models have been trained with batches of size 256, as in (Wang et al., 2019). PNs’s episodic batch setup uses  $a=16$ , as it is the highest performing one.

not enforcing a certain amount of images per class can cause many classes to have a single representative example (which cannot contribute towards the number of positive pairs). These changes affect all our methods and baselines: NCA, Prototypical Networks (with both old and new batch setup), and SimpleShot (Wang et al., 2019).

**Projection network.** Similarly to (Khosla et al., 2020; Chen et al., 2020a), we also experimented (for both PNs and NCA) with a *projection network* (but *only* for the comparison of Sec. 4.4). The projection network is a single linear layer  $A \in \mathbb{R}^{M \times P}$  that is placed on top of  $f_\theta$  at training time, where  $M$  is the output dimension of the neural network  $f_\theta$  and  $P$  is the output dimension of  $A$ , which can be considered as a hyperparameter. The output of  $A$  is only used during training. At test time, we do not use the output of  $A$  and directly use the output of  $f_\theta$ . For CIFAR-FS and *tieredImageNet*, we found this did not help performance. For *miniImageNet* however we found that this improved performance, and we set  $P = 128$  (which worked best for both PNs and NCA). Note that this is not an unfair advantage over other methods. Compared to SimpleShot (Wang et al., 2019) and other simple baselines, we actually use fewer parameters without the projection network (effectively making our ResNet12 a ResNet11) since they use an extra fully connected layer to minimise cross-entropy during pre-training.

## A.5 Choice of hyperparameters

During the experimental design, we wanted to ensure a fair comparison between the NCA and PNs. As a testimony of this effort, we obtained very competitive results for PNs (see for example the comparison to recent papers where architectures of similar capacity were used (Wang et al., 2019; Chen et al., 2019)). In particular:

- We always use the normalisation strategy of Wang et al. (2019), as it is beneficial also for PNs.
- Unless expressly specified, we always used PNs’ 5-shot model, which in our implementation outperforms the 1-shot model (for both 1-shot and 5-shot evaluation). Instead, (Snell et al., 2017) train and tests with the same number of shots.
- Apart from the episodes hyperparameters of PNs, which we did search and optimise over to create the plots of Fig. 2, the only other hyperparameters of PNs are those related to the training schedule, which are the same as the ones used for NCA. To set them, we started from the simple SGD schedule used by Wang et al. (2019) and only marginally modified it by increasing the number of training epochs to 120, increasing the batch size to 512 and setting weight decay and learning rate to  $5e-4$  and 0.1, respectively. As a sanity check, we trained both the NCA and PNs with the exact training schedule used by Wang et al. (2019). Results are reported in Table 6, and show that the schedule we used for this paper is considerably better for both PNs and NCA. In general, we observed that the modifications were beneficial for both NCA and PNs, and improvements in performance in NCA and PNs were highly correlated. This is to be expected given the high similarity between the two methods and losses.

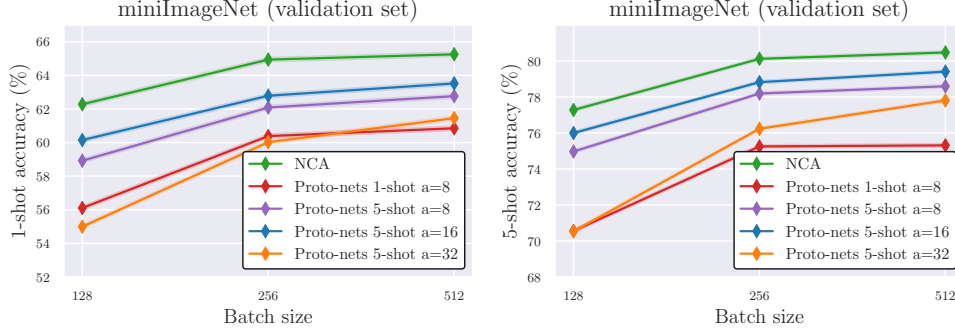


Figure 6: 1-shot and 5-shot accuracies on the validation set of *miniImageNet* for different batch sizes. Models are trained using NCA or PNs with different configurations: 1-shot with  $a = 8$  and 5-shot with  $a = 8, 16$  or  $32$ . Reported values correspond to the mean accuracy of five models trained with different random seeds. Please see Sec. 4.2 for details.

## A.6 Additional results for Sec. 4.2

Fig. 6 complements the results of Fig. 2 from Sec. 4.2

## A.7 Details about number of pairs description of Section 3.3

In this section, we demonstrate that the total number of training pairs that NCA can exploit within a batch is always strictly superior to the one exploited by the episodic batch strategy used by Prototypical Networks.

To ensure we have a “valid” episodic batch with a nonzero number of both positive and negative distance pairs, we assume that  $n, m \geq 1$ , and  $w \geq 2$ .

Below, we show that the number of positives for NCA, i.e.  $\binom{m+n}{2}w$ , is always greater or equal than the one for PNs, which is  $mnw$ :

$$\begin{aligned}
 \binom{m+n}{2}w &= \frac{(m+n)!}{2!(m+n-2)!}w \\
 &= \frac{1}{2}(m+n)(m+n-1)w \\
 &= \frac{1}{2}(m^2 + 2mn - m + n^2 - n)w \\
 &= \frac{1}{2}(m(m-1) + 2mn + n(n-1))w \\
 &\geq \frac{1}{2}(2mn)w = wmn.
 \end{aligned}$$

Similarly, we can show for negative distance pairs that  $\binom{w}{2}(m+n)^2 > w(w-1)mn$ :

$$\begin{aligned}
 \binom{w}{2}(m+n)^2 &= \frac{w!}{2!(w-2)!}(m^2 + 2mn + n^2) \\
 &= \frac{1}{2}w(w-1)(m^2 + 2mn + n^2) \\
 &> \frac{1}{2}w(w-1)(2mn) \\
 &= w(w-1)mn.
 \end{aligned}$$

This means that the NCA can always rely on at least the same number of positive distances and strictly more negative distances than Prototypical Networks. Specifically, the total number of *extra* pairs that NCA can exploit is  $\frac{w}{2}(w(m^2 + n^2) - m - n)$ .

rank	method	# pos	# neg	# total pairs
1	NCA	1792	129024	130816
2	5-shot $a=16$	1760	54560	56320
3	5-shot $a=8$	960	60480	61440
4	5-shot $a=32$	2160	32400	34560
5	1-shot $a=8$	448	28224	28672

Table 7: Number of positive and negative gradients contributing to the loss which NCA and the different variants of PNs from the experiment of Fig. 2 can exploit (considering a batch of size 512).

### A.8 Details about number of pairs description of Section 4.2

In Table 7 we plot the number of positives and negatives for NCA and the different episodic configurations of PNs, to see whether the difference in performance can be explained by the difference in the number of distance pairs that can be exploited in a certain batch configuration. This is often true, as the ranking can almost be fully explained by the number of total pairs in the right column. However, there are two exceptions to this: 5-shot with  $a=16$  and 5-shot with  $a=8$ .

To understand this, we can see that the number of positive pairs is much higher for  $a=16$  than for  $a=8$ . Since the positive pairs constitute a less frequent (and potentially more informative) training signal, this can explain the difference. The  $a=32$  variant has an even higher number of positives than  $a=16$ , but the loss in performance there could be explained by a drastically lower number of negatives, and by the fact that the number of ways used during training is lower. So, while indeed generally speaking the higher number of pairs the better (which is also corroborated by Fig. 3, where moving right on the x-axis sees higher performance for both NCA and PNs), one should also consider how this interacts with the positive/negative balance and the number of classes presents within a batch.